A. Gritsenko

Doctor
South Ural State Agrarian University
Department of Machine-Tractor
Fleet Operation
Russia

V. Shepelev

Ph. D
South Ural State University
Automobile and Tractor Faculty
Russia

A. Burzev

Ph. D
Gorbachev Kuzbass State Technical
University
Department of Mining and
Technosphere Safety
Russia

B.K. Kaliyev

Department of Mechanical Engineering
NLC A. Baitursynov Kostanay Regional
University
Kazakhstan

The Development of a Method for Diagnosing Internal Combustion Engines Based on Acceleration and Rundown Characteristics

The paper proposes applying a precise and low-cost internal combustion engine (ICE) diagnostic method based on acceleration and rundown characteristics. We developed an engine test stand based on and selected diagnostic tools to record acceleration-rundown parameters: a DBD-4 gasoline engine loader and USB Autoscope 4. We established that the injector feed rate significantly affects acceleration time, while the wear of the cylinder-piston group (CPG) significantly affects the acceleration time of the ICE crankshaft. When CPG wear was 28%, acceleration time increased to 15 s, and when the wear was 5% – to 3s. The rundown time significantly depends on the outlet resistance and increases with an increase in the degree of CPG wear. Applying the developed method reduced the fuel consumption of the test engine by 21%.

Keywords: engine, acceleration-rundown, diagnostics, failure.

1. INTRODUCTION

The current stage of scientific and technological deve–lopment provides various methods for diagnosing internal combustion engines: based on lubricating oil parameters [1–5], the vibration spectrum analysis [6–11], instantaneous rotation speed analysis, fuel consum–ption, instantaneous measurement of the angular crank-shaft acceleration [12, 13], etc. There are numerous models, theories, and algorithms [14] for fault diag-nostics, including neural networks [15, 16], simulation modeling [17, 18], wavelet analysis and transform [6, 19, 20], heredity algorithm [21], fuzzy algorithms [22], and more. Researchers primarily focus on the deve–lopment and implementation of in-place diagnostic methods since identifying minor faults can often be resource-intensive [23, 24].

Notably, there are effective methods of vibro–acoustic ICE diagnostics. Acoustic diagnostics offer the advantage of simple and quick measurements. Diag–nostic charts based on the measured acoustic spectrum [7–11] can be useful for assessing the technical con–dition of the tested engine. The main disadvantage of this method is that background noise and other noise sources that do not affect the engine operation must be accounted for and removed.

The continuous wavelet transform method [6, 20] and artificial neural networks [16] are proposed to de–tect signals caused by damaged elements hidden in broadband background noise. Artificial neural networks are also utilized to predict engine performance and ex–haust emissions with an accuracy of over 95% [16]. The

use of neural networks for automated combustion mis–fire diagnostics in ICE is presented in [22], where the authors diagnose the severity and location of damage.

The instantaneous angular acceleration method of diagnosing ICE allows checking the technical condition of a group of cylinders but does not provide complete information on the engine power. This diagnostic method can identify failures related to combustion and other issues affecting gas pressure in the cylinders by analyzing instantaneous velocity [13, 25]. Measuring instantaneous speed requires highly sensitive equipment and analysis of large volumes of data. Recent research on instantaneous angular velocity has focused on the post-processing of instantaneous angular velocity signals using wavelet analysis and neural network analysis [26-28].

Frictional diagnostics is an in-site diagnostic method that utilizes lubricating oil as a source of information about processes and changes in mechanical systems. However, the costs of repair often exceed the inves–tment in preventive maintenance and special equipment is required [1, 3]. Selecting the necessary parameters to classify wear particles can be laborious and involve time-consuming calculations. Despite the labor costs associated with this method, it does not guarantee suf–ficient reliability that the particles belong to the selected class. In [2], the authors proposed a classification method based on dissimilarity indicators.

There is no doubt that all the methods for diagnosing and assessing the technical condition of internal com–bustion engines are effective and precise. However, operating companies may not always have access to specific diagnostic tools. Therefore, the main goal of technical diagnostics in automobile engines is to provide an easy and accurate method for assessing technical conditions.

The article proposes a universal diagnostic method based on acceleration-rundown characteristics. This

method is implemented through continuous monitoring of the diagnosed systems. To record acceleration-rundown parameters, a DBD-4 gasoline engine loader (to provide test modes) and a USB Autoscope 4 (Posto–lovsky's electronic multichannel oscilloscope) [24, 29] were selected as diagnostic tools. The output control parameters are the time parameters of acceleration-rundown and the total number of crankshaft revolutions before the ICE stops [30].

Scientific merits of the paper:

• the correlation between the acceleration and dece–leration of the vehicle's ICE and the condition of the fuel delivery system has been established;

• an analytical description of the changes in tech–nical and economic indicators during the implemen–tation of the developed diagnostic method is presented;

•a diagnostic algorithm for the fuel delivery system has been developed based on the derived correlations of the ICE acceleration and deceleration with the condition of the fuel delivery system.

The contribution to engineering practice includes:

• justification of the methodology for test diag–nostics of the ICE fuel delivery system based on moni–toring the characteristics of acceleration and dece–ration;

• development of mode selection and diagnostic par–ameters that accurately describe the technical condition of the fuel delivery system;

• presentation of experimental data, the comparison of which enables the assessment of the technical con–dition of the ICE fuel delivery system;

• development of recommendations for monitoring the technical condition of the fuel delivery system, ta–king into account the influence of the technical condi–tion of other systems.

The practical application includes:

• Development of a method and technology for diagnosing the fuel delivery system based on acce–leration and deceleration characteristics. This allows for the timely elimination of failures and malfunctions of engine system elements within the service enterprise;

• Automotive service organizations can utilize the research results to determine the technical condition of the fuel delivery system.

2. THEORETICAL RESEARCH

We chose the method of free acceleration to establish the relationship between the technical condition of the ICE and the acceleration-rundown parameters. The acceleration condition can be met by an additional fuel supply and by providing power exceeding friction horsepower. Thus, we can write the equation for moment balance for the free acceleration condition:

$$M_i - M_t - M_\varepsilon = 0 \qquad (1)$$

where M_i is the indicated moment (N·m); M_t is the frictional moment (N·m); M_ε is the moment connected with an increase in the kinetic energy when the fuel supply increases (N·m).

Let us write M_ε through separate components; then, we will obtain:

$$J \frac{d\omega}{dt} = M_i - M_t \qquad (2)$$

where J is the moment of inertia reduced to the axis of the ICE crankshaft (N·m²); $dt/d\omega$ is the instantaneous acceleration value of the ICE crankshaft (rad/s²).

An analysis of (1) and (2) shows that during acce–leration, the kinetic energy increases due to an increase in the indicated power. Depending on certain combi–nations of factors, the increase in indicated power can exceed or fall short of the nominal value, leading to faster or slower acceleration. Several significant factors influence acceleration speed, including the servicea–bility of the elements of ignition, fuel supply, gas distribution, intake, CPG, and exhaust systems. It is worth noting that the introduction of complex exhaust systems, such as catalytic converters, has significantly increased the occurrence of failures that affect acce–leration and rundown time. However, not all the afo–rementioned factors impact the rundown of the ICE crankshaft. Previous studies have established that rundown is influenced by the condition of the exhaust system, CPG, and the gas distribution system – anything that can affect the intake and exhaust resistance. Taking into account the above provisions, acceleration can be represented by the general expression:

$$\varepsilon(\omega) = f\left(s_1; s_2; s_3; s_4; s_5; s_6 \ldots s_i\right) \qquad (3)$$

where s_1 is the degree of CPG wear; s_2 is the technical condition of the gas distribution system; s_3 is the tech–nical condition of the ignition system; s_4 is the technical condition of the intake system; s_5 is the technical con–dition of the exhaust system; and s_6 is the technical condition of the fuel supply system.

However, upon examining the weight of each factor in equation (3), it becomes evident that individual indi–cators significantly differ in terms of their degree of influence. The limiting value of one parameter has a much greater impact on acceleration compared to ot–hers. Furthermore, analyzing ICE acceleration with all cylinders operational or with individual cylinders dis–abled can significantly enhance the diagnostic process by providing more informative data. This is particularly important for multi-cylinder ICEs, where the specific gravity of each component is smoothed out by the influence of other properly functioning objects.

Several studies have shown that acceleration is usually much faster than the rundown process for most of the operated ICEs. However, acceleration and run–down conditions are essential: the speed at which the throttle valve opens, the reaction rate of the fuel supply system, and other factors.

Several publications mention the concept of cycle time for free acceleration and deceleration. We will mainly present the results of acceleration and decele–ration separately.

The sum of the acceleration and rundown times is determined by the expression:

$$t_c = t_a + t_r = \frac{\Delta\omega}{\varepsilon_a} + \frac{\Delta\omega}{\varepsilon_r} = \Delta\omega \frac{\varepsilon_a + \varepsilon_r}{\varepsilon_a \cdot \varepsilon_r} \qquad (4)$$

where t_a is the point of free acceleration (s); t_r is the point of free rundown (s); $\Delta\omega$ is the increment or the degree of reduction of the ICE crankshaft speed (pro–vided that the same values of the greatest speeds are being considered during acceleration and rundown) (rpm); ε_a is the acceleration value during acceleration (rad/s^2); ε_r is the deceleration value during rundown (rad/s^2).
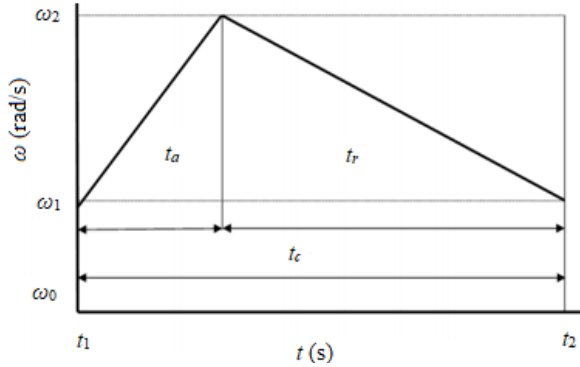
The cycle time can be presented in a graph (Fig. 1)

Figure 1. Cycle time during the evaluation of acceleration parameters.

Let us consider the theory of acceleration and run–down and the calculation of cycle parameters. If the ICE fully complies with the regulations and technical documentation, the cycle time can be written as t_{c0}:

$$t_{c_0} = \Delta\omega \frac{\varepsilon_a + \varepsilon_r}{\varepsilon_a \cdot \varepsilon_r} \quad (5)$$

However, with the appearance of faults in ICE systems and parts, the parameters of (5) will change. Taking into account changes to technical conditions, let us write cycle time as $t_{c\alpha}$ and $t_{c\beta}$. In the first case, the technical condition of the ICE systems affected the acceleration time, in the second case – the rundown time. The equa–tions will be as follows:

$$t_{c_\alpha} = \Delta\omega \frac{\alpha\varepsilon_{a_0} + \varepsilon_{r_0}}{\alpha\varepsilon_{a_0} \cdot \varepsilon_{r_0}} \quad (6)$$

$$t_{c_\beta} = \Delta\omega \frac{\varepsilon_{a_0} + \beta\varepsilon_{r_0}}{\beta\varepsilon_{a_0} \cdot \varepsilon_{r_0}} \quad (7)$$

where α characterizes the change in the time compo–nents of acceleration and β characterizes the change in the time components of rundown.

Let us consider a situation in which the time para–meters of acceleration have changed during operation, not taking into account the rundown because it remained in the same time frame. Then, we can write the condition in the form of the coefficient K_{tc}:

$$K_{tc} = \frac{t_{c0}}{t_{c\alpha}} = \frac{\varepsilon_a + \varepsilon_r}{\varepsilon_a \cdot \varepsilon_r} \times \frac{\alpha\varepsilon_{a_0} + \varepsilon_{r_0}}{\alpha\varepsilon_{a_0} \cdot \varepsilon_{r_0}} = \frac{\alpha(\varepsilon_{a_0} \cdot \varepsilon_{r_0})}{\alpha\varepsilon_{a_0} + \varepsilon_{r_0}} \quad (8)$$

If failures affecting acceleration and rundown appear simultaneously (when $\alpha \neq 1$ and $\beta \neq 1$), (8) can be written as follows:

$$K_{tc} = \frac{\alpha\beta(\varepsilon_{a_0} \cdot \varepsilon_{r_0})}{\alpha\varepsilon_{a_0} + \beta\varepsilon_{r_0}} \quad (9)$$

A disadvantage of utilizing this coefficient to assess the technical condition of ICE is the ambiguity that can result from the superimposition of several mutually exclusive failures. As diagnostic practice shows, it is more convenient to evaluate acceleration and rundown time separately rather than comparing them with the tabular values for new ICEs.

Let us present an example of applying the method with alternating acceleration-rundown cycles for a ZMZ-4062 engine (Fig. 2).
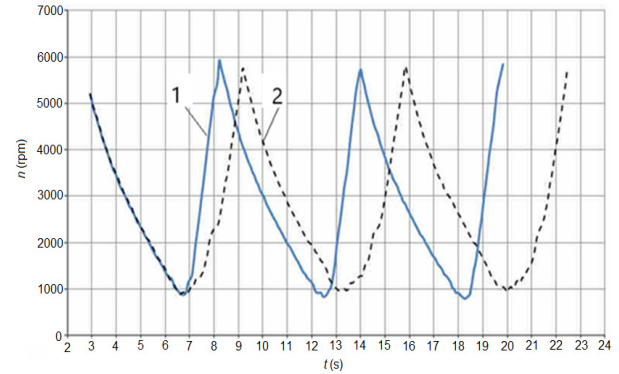

Figure 2. The acceleration-rundown characteristic of a ZMZ-4062 engine: (1) 1.6 mm^2 total CPG wear, 300 kPa fuel pressure in the fuel rail; (2) 1.6 mm^2 total CPG wear, 250 kPa fuel pressure in the fuel rail.

An analysis of the characteristics (Fig. 2) shows that a decrease in the fuel supply (when the pressure in the fuel rail varies from 300 to 250 kPa) leads to an increase in acceleration time by almost 1 second. At the same time, the rundown time parameters remain unchanged.

The characteristics of the acceleration-rundown pro–cess are also illustrative (Fig. 3)
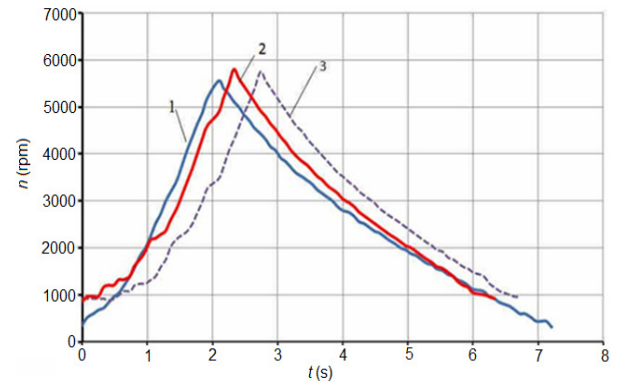

Figure 3. The acceleration-rundown characteristic of a ZMZ-4062 engine with varying combinations of failures: (1) 0.75 mm^2 total CPG wear, 300 kPa fuel pressure in the fuel rail; (2) 2.35 mm^2 total CPG wear, 250 kPa fuel pressure in the fuel rail; (3) 2.35 mm^2 total CPG wear, 200 kPa fuel pressure in the fuel rail.

Figure 3 shows that in the first variation of factors, acceleration takes at least 2.13 s. In the second case, acceleration is extended to 2.34 s. In the third case, acceleration takes significantly longer – 2.78 s. The disadvantage of the obtained data is that it is difficult to relate the fuel rail's pressure to the fuel injector's actual flow rate. However, the dynamics of the increase in acceleration time clearly characterize the decrease in the capacity of the electromagnetic injectors. At the same time, the influence of CPG wear on the rundown pro–

cess is not noticeable. When the rundown starting points of all three graphs overlap, the slope and the rundown are the same, although previous diagnostic measure–ments showed that ICE rundown time increases along with an increase in CPG wear.

Acceleration parameters are an important aspect, particularly the position of the throttle valve during acceleration and subsequent rundown. Let us present our results showing four positions of the throttle valve (Fig. 4).
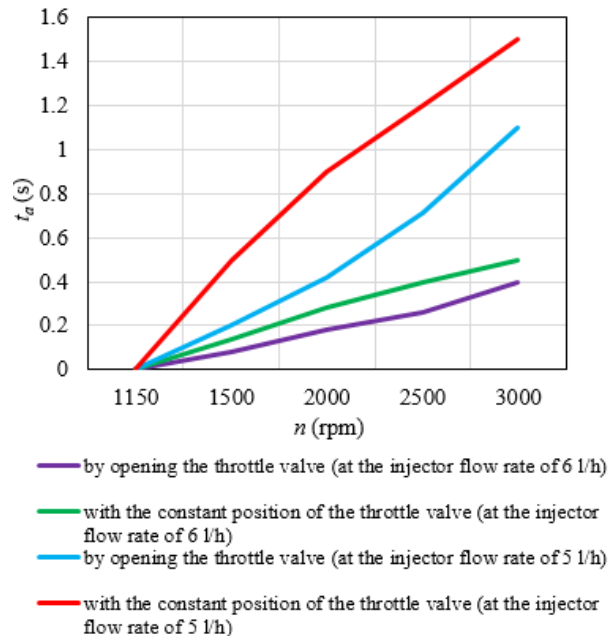

Figure 4. Acceleration characteristics at different positions of the throttle valve.

Figure 4 shows that each combination of factors results in different acceleration times. The slowest acce–leration is obtained when the throttle position remains unchanged with the flow rate of the electromagnetic injector of 5 l/h. Moreover, the number of revolutions is increased by an increase in injection duration within the greatest possible value limits. However, Figure 4 shows that with an increase in the injector flow rate to 6 l/h, acceleration time decreases.

3. METHODS

For our studies, we developed an engine test stand, cha–nged the capacity of fuel injectors using a set of drills and pads with calibrated bores, and used a DBD-4 gaso–line engine loader (for setting test modes) and USB Autoscope 4 (Postolovsky's oscilloscope) as diagnostic tools [29, 30].

We modified the flow section of the nozzles for the experimental set of electromagnetic injectors. To inc–rease the outlet section and, therefore, the feed rate, the feed orifice (channel) located behind the injector valve was drilled using the selected drill diameters. To reduce the outlet section of the electromagnetic injector, we installed specially prepared washers with reduced orifices.

A test stand based on the ZMZ-4062 engine was used in our study. The ZMZ-4062 engine is a 4-cylinder, 16-valve injection gasoline engine with fuel

injection in front of the inlet valve; the piston stroke is 86 mm, the cylinder diameter is 92 m, the cylinder operation mode is 1-3-4-2, the environmental standards are Euro-4 (Fig. 5).
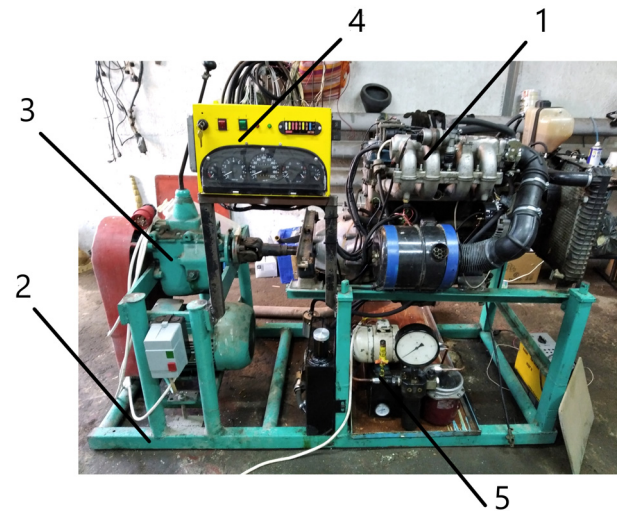

Figure 5. Experimental setup: 1– ZMZ-4062 engine; 2– stand frame; 3– electric transmission; 4– remote control; 5– oil hydraulic system for turbocharger power supply.

Measurement instruments are connected to the control points, and all processes are recorded in the form of data oscillograms. The obtained oscillograms are numbered in accordance with the sequence of experimental data processing. They are then processed using applied mathematical statistics software packages.

A USB Autoscope 4 (Postolovsky's oscilloscope) was used to control the acceleration and rundown times and the number of revolutions made by the crankshaft until the complete stop of the ICE. During our study, the ICE speed was set at a certain level. The start of the oscillogram display using the USB Autoscope 4 was ensured simultaneously with the ongoing operation of the engine (Fig. 6).

After achieving a constant rotational speed of the engine crankshaft, the moment was ensured for its fixation on the oscillogram (Fig. 6). At the specified re–porting moment, the fuel injection pulses (spark generation) were disabled, and the oscillogram captu–ring the deceleration process was recorded from the be–ginning until the complete stoppage of the engine crankshaft (Fig. 7).

During the engine start-up, the oscillogram display using the USB Autoscope 4 was initiated simultane–ously. Afterward, the initial value of the engine crank–shaft rotational speed was established (Fig. 7). Fol–lowing this, the recording was started, after which the ignition was simultaneously turned off, and the dece–leration of the engine crankshaft was recorded until its complete stoppage (Fig. 8).

After the complete stoppage of the engine, the recording was terminated, and the current time segment was saved in the memory of the computer device connected to the USB Autoscope 4. As can be seen from Fig. 8, the deceleration time amounted to 3.81 seconds. Additionally, the total number of revolutions of the engine crankshaft until its complete stoppage is calculated based on the recorded oscillogram.
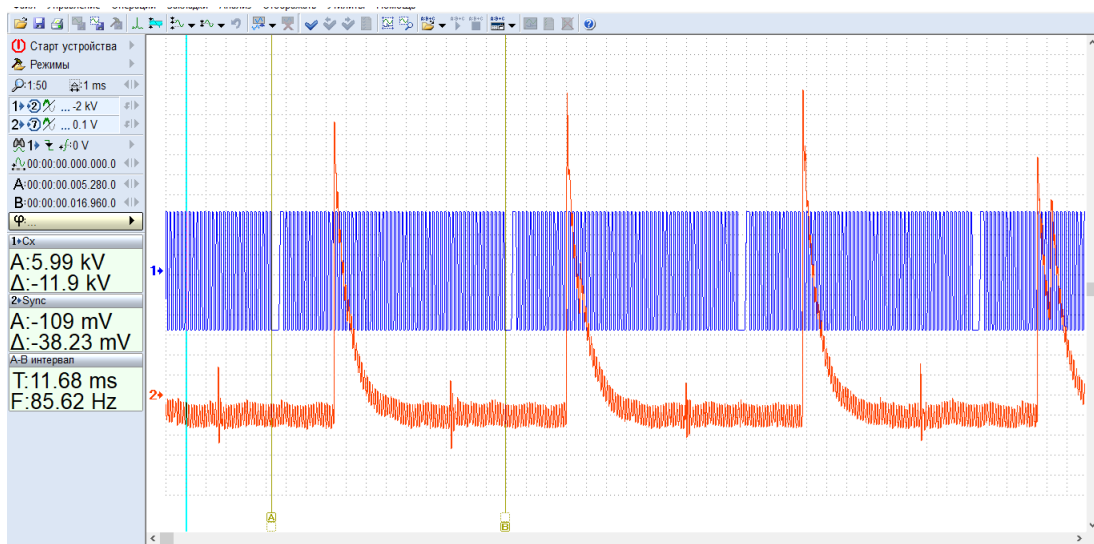
Figure 6. A recorded current sweep of the USB Autoscope 4 oscillogram: (1) The change in signal of the crankshaft position sensor at a stable constant speed of the ICE crankshaft; (2) The change in the signal of the primary circuit of the ignition system.
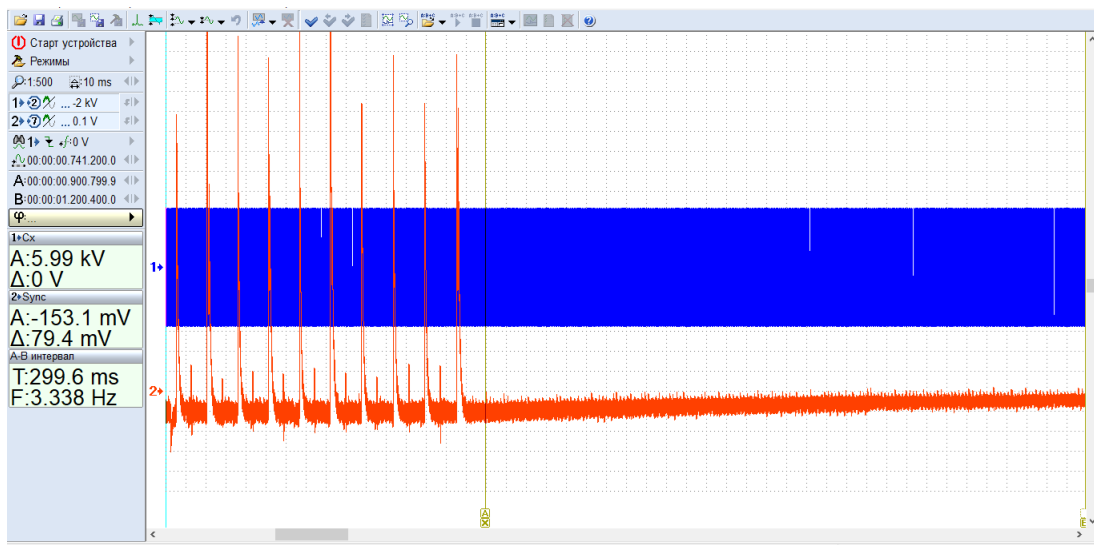

Figure 7. A recorded current sweep of the USB Autoscope 4 oscillogram: (1) The change in the signal of the crankshaft position sensor until the complete stoppage of the engine; (2) The change in the signal of the primary circuit of the ignition system (moment of ignition pulse deactivation).
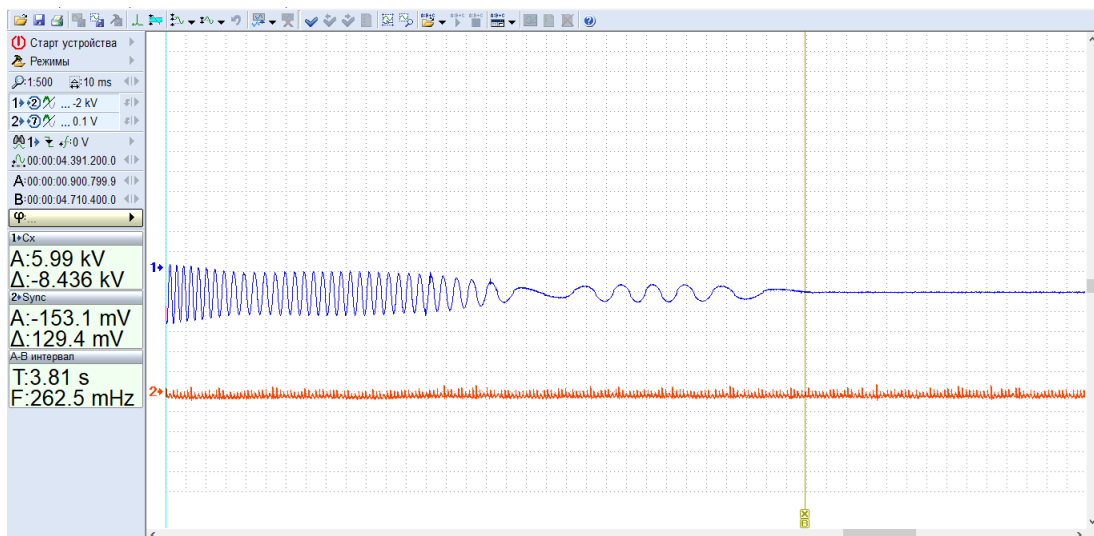

Figure 8. A recorded current sweep of the USB Autoscope 4 oscillogram: (1) The variation of the signal from the crankshaft position sensor until the complete stoppage of the engine; (2) The change in the signal of the primary circuit of the ignition system (ignition pulses turned off)

4. RESULTS

Let us consider the experimental dependence of accele–ration time (t) on injector capacity ($\Delta\mu f$) under various acceleration conditions (Fig. 9).
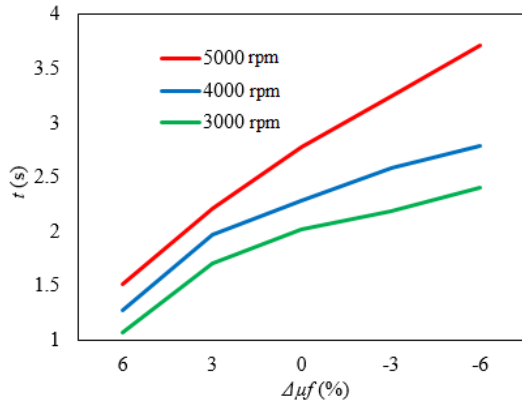

Figure 9. The dependence of acceleration time on injector capacity.

The gas pedal is used to set the initial ICE crank–shaft speed to carry out measurements on an operating engine. Upon reaching the given initial ICE crankshaft speed, the gas pedal is fixed, and stable readings of the ICE crankshaft speed are achieved.

The greatest difference in the acceleration values (Fig. 9) is observed when injector capacity is reduced by -6%. However, the slope angle of the acceleration time dependencies is somewhat different. For larger initial ICE crankshaft speeds, the slope angle is larger. A significant increase in acceleration time is observed when injector capacity is -6% at high crankshaft speeds. This is caused by the depletion of the fuel-air mixture. After +6% injector capacity, the slope angle of the dependences is increased and coincides for all three rundown variants.

Acceleration time changes linearly within the variation range of injector capacity from +3% to -6%.

The experimental dependence of rundown time on CP wear under various rundown starting conditions (Fig. 10) can serve as an example of the dependence of the rundown time on the technical condition of the ICE elements.

Figure 10 shows that with an increase in CPG wear, the rundown time increases significantly, and when the critical point of wear (28%) is reached, the ICE does not reach the specified crankshaft speed (stalls), which is caused by the leakage of the fuel-air mixture.
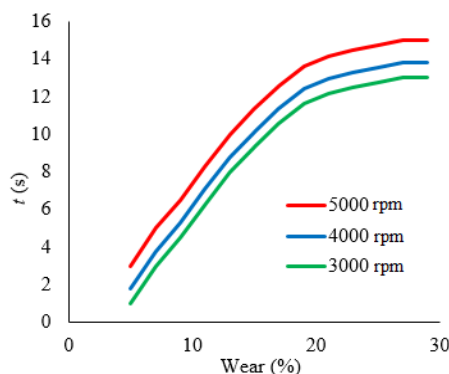

Figure 10. The dependence of rundown time on CPG wear.

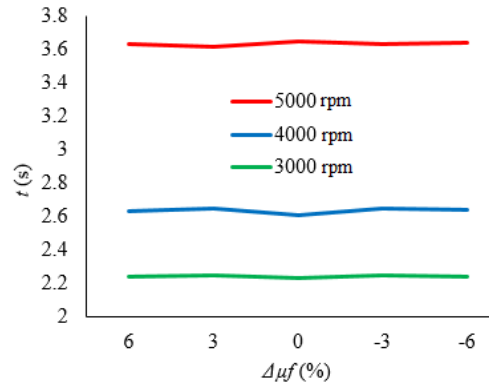Let us consider the experimental dependence of the rundown time on injector capacity (Fig. 11).

Figure 11. The dependence of the rundown time on injector capacity.

Figure 11 shows that the greatest difference in the rundown time values is observed when injector capacity is increased by 6%. Within the variation range of injector capacity from +6% to -6%, the rundown time varies linearly. No critical points were found. Based on this assumption, we can conclude that the rundown time value does not depend on the change in injector capacity within the range from +6% to -6%.

The experimental dependence of the rundown time t on the equivalent diameter of the exhaust pipe (Fig. 12) can serve as an example of the dependence of the rundown time on the technical condition of the ICE elements.
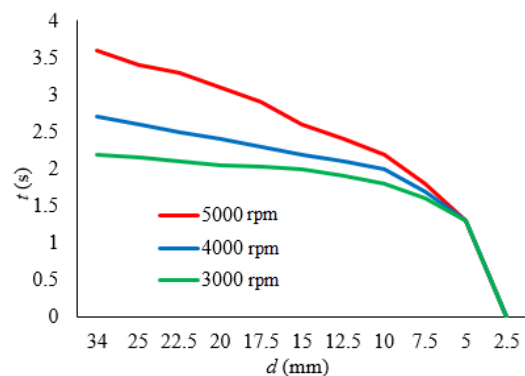

Figure 12. The dependence of the rundown time on the equivalent diameter of the exhaust pipe.

The greatest difference in the values of the rundown time (Fig. 12) is observed at the equivalent diameter of the outlet pipe d=34 mm. However, the slope angle of the rundown time dependences is somewhat different: for large initial ICE crankshaft speeds, the slope angle is larger. In the range from d=34 mm to 10 mm, the rundown time varies linearly. After d=10 mm, the slope angle of the dependences sharply increases and coin–cides for all the three mentioned rundown variations. However, at d=10 mm, the critical option of the exhaust tract resistance is observed, after which it is impossible to set the initial ICE crankshaft speed at 5000, 4000, and 3000 rpm. The balance point is observed at a lower speed. Our experiments have shown that the zone of equivalent cross-sections less than 10 mm is critical. After this point, ICE operation is complicated or impossible.

The experimental dependence of rundown time on CPG wear (Fig. 13) can serve as an example of the dependence of rundown time on the technical condition of the ICE elements.
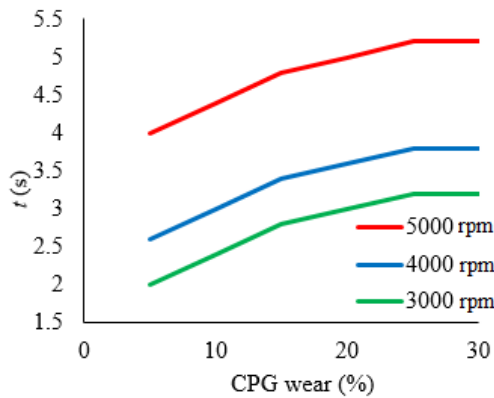

Figure 13. The dependence of rundown time on CPG wear.

Figure 13 shows that with an increase in CPG wear, rundown time increases significantly.

The dependence of acceleration time on the initial ICE crankshaft speed at various values of injector capacity is illustrative (Fig. 14).
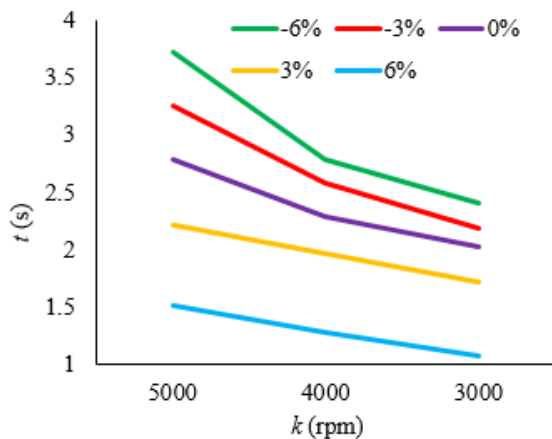

Figure 14. The dependence of acceleration time on the initial ICE crankshaft speed with various changes to fuel injector capacity.

With a decrease in the diameter of the injector spray nozzle (Fig. 14), ICE acceleration time increases. The increasing dynamics of acceleration time are the most significant at the earlier stages of increasing resistance (from -3% to -6%). The difference in acceleration time between two adjacent dependencies is $\Delta t = 0.3$ s with a decrease in the equivalent cross-section from 0% to -3%. As injector capacity decreases below -3%, the decrease in the rundown time becomes less noticeable. The rundown time difference between two adjacent dependencies becomes less $\Delta t = 0.3$ s. At + 3% to -6% injector capacity at high crankshaft speeds, we observe a significant increase in acceleration time caused by the depletion of the fuel-air mixture.

Let us consider the dependence of the rundown time on the initial ICE crankshaft speed at various values of injector capacity ($\Delta \mu f$) (Fig. 15).

As Fig. 15 shows, we did not observe the maximum difference between the values of the rundown time from the initial ICE crankshaft speed at different injector

capacity values. The actual rundown time varies linearly at +6% to -6% injector capacity. No critical points were found. Based on this assumption, rundown time does not depend on the changes in injector capacity within the range from +6% to -6%.
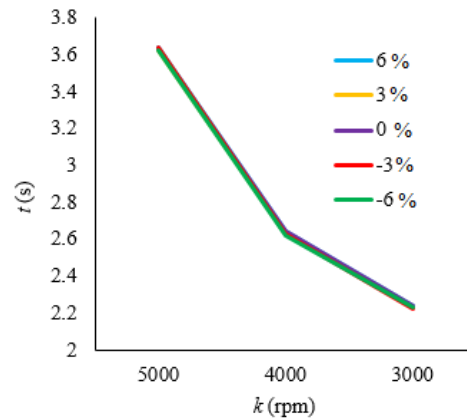

Figure 15. The dependence of the rundown time on the initial ICE crankshaft speed at various values of changes in injector capacity.

The experimental dependence of the rundown time on the initial ICE crankshaft speed at different values of the equivalent diameter of the exhaust pipe (Fig. 16) can serve as an example of the dependence of the rundown time on the technical condition of ICE elements.
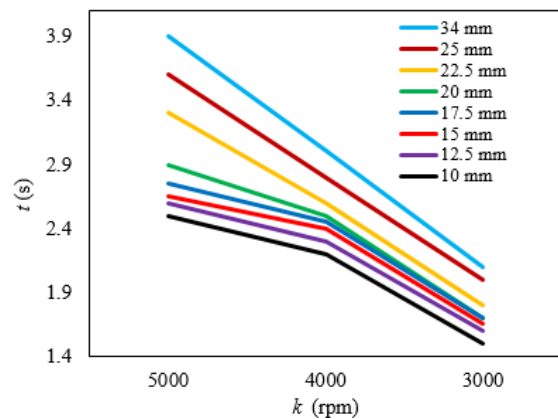

Figure 16. The dependence of the rundown time on the initial ICE crankshaft speed at different values of the equivalent diameter of the exhaust pipe.

As exhaust tract resistance increases, ICE rundown time decreases (Fig. 16). The decreasing dynamics of the rundown time are most significant at the earlier stages of increasing resistance. The difference in the rundown time between two adjacent dependencies is $\Delta t = 0.3$ s with a decrease in the equivalent cross-section from 34 to 25 mm. As the equivalent diameter of the outlet pipe decreases below $d=20$ mm, the decrease in the rundown time becomes less noticeable. The rundown time difference between two adjacent dependencies becomes less $\Delta t = 0.1$ s.

An important diagnostic parameter is the total number of revolutions before the engine stops (Fig. 17).

With +6% to -6% injector capacity (Fig. 17), the dependence is linear. No critical points were found. Based on this assumption, we can conclude that changes in injector capacity do not affect the value of the rundown time.
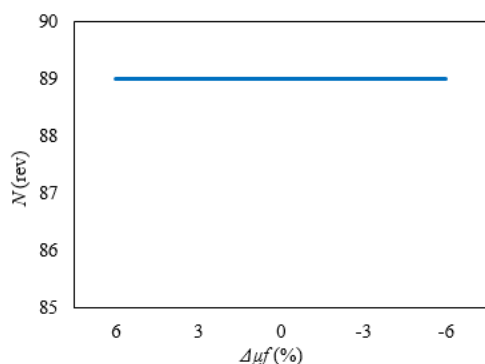
Figure 17. The dependence of the total number of revolu–tions before the engine stops on injector capacity provided that the rundown begins from 5000 rpm.

We examined the experimental dependence of the total number of revolutions before the engine stops on the equivalent diameter of the exhaust pipe, provided that the rundown begins from 5000 rpm (Fig. 18). This can serve as an example of the dependence of rundown time on the technical condition of ICE elements.
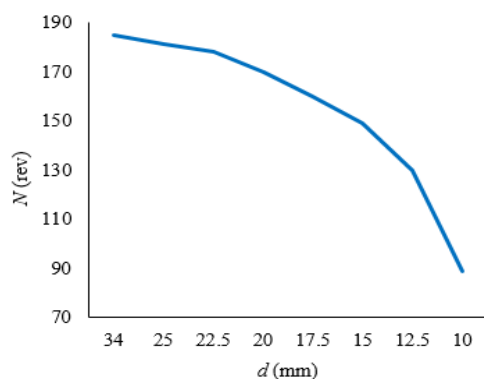

Figure 18. The dependence of the total number of revolutions before the engine stops on the equivalent diameter of the exhaust pipe provided that the rundown begins from 5000 rpm.

Figure 18 shows that in the initial variation range of the equivalent diameter of the outlet pipe d=34…15 mm, the dependence is almost linear. However, below d=15 mm, the dependence dynamically bends down–ward, and at 10 mm, we do not observe the condition for the beginning of the rundown from 5000 rpm. In other words, the engine no longer picks up such speed. As exhaust tract resistance increases, the stable possible crankshaft speed at the beginning of the rundown decreases.

5. CONCLUSION

For our study, we developed a research methodology that involved designing an engine test stand, modifying fuel injector capacity, and creating a device to simulate exhaust system resistance.

We discovered that acceleration time can serve as a sensitive diagnostic parameter for assessing the tech–nical condition of the fuel supply system. When analyzing the experimental relationship between accele–ration time on injector capacity (provided that the rundown begins from 5000 rpm, 4000 rpm, and 3000 rpm), the most significant difference in acceleration time

values was observed at injector capacity ranging from –3% to –6%. Based on numerous experiments, it was determined that –3% injector capacity is the critical point beyond which the operation ICE becomes challenging or impossible due to a substantial depletion of the fuel-air mixture. Changes in the technical condition of the fuel system did not affect the rundown time. Additionally, by employing this method, we achieved a 21% reduction in fuel consumption for the tested engine.

REFERENCES

[1] Glos, J.: Tribologic methods used for an engine diagnostics, in: *Proceedings of the 6th International Conference on Intelligent Technologies in Logistics and Mechatronics Systems*, 5-6.10.2011, Panevezys, pp. 9-13.

[2] Podsiadlo, P., Stachowiak, G.W.: Development of advanced quantitative analysis methods for wear particle characterization and classification to aid tribological system diagnosis, Tribology International, Vol. 38, No. 10, pp. 887-897, 2005.

[3] Stodola, J.: Tribo-technical diagnostics of combustion engines, in: Proceedings *of Eighteenth FISITA Congress - The Promise of New Technology in the Automotive Industry*, 7-11.05.1990, Torino, pp. 271-281.

[4] Siegel, J., Bhattacharyya, R., Deshpande, A., Sarma, S.: Vehicular engine oil service life characterization using on-board diagnostic (OBD) sensor data, in: *Proceedings of 13th IEEE SENSORS Conference*, 2-5.11.2014, Valencia, paper 6985355, pp. 1722-1725.

[5] Kuti, R., Könczöl F., Csapó L., Földi L., Tóth Á.D.: Detection of the possible engine damages in case of a continuous track military vehicles with tribological investigations, FME Transactions, Vol. 50, No. 3, pp. 526 - 534, 2022.

[6] Czech, P., Wojnar, G., Burdzik, R., Konieczny, Ł., Warczek, J.: Application of the discrete wavelet transform and probabilistic neural networks in IC engine fault diagnostics, Journal of Vibroengineering, Vol. 16, No. 4, pp. 1619-1639, 2014.

[7] Komorska, I.: Diagnostic-oriented vibroacoustic model of the reciprocating engine, Solid State Phenomena, Vol. 180, pp. 214-221, 2012.

[8] Deptuła, A., Kunderman, D., Osiński, P., Radziwanowska, U., Włostowski, R.: Acoustic diagnostics applications in the study of technical condition of combustion engine, Archives of Acoustics, Vol. 41, No. 2, pp. 345-350, 2016.

[9] Winklhofer, E.: Optical access and diagnostic techniques for internal combustion engine development, in: *Proceedings of SPIE - The International Society for Optical Engineering*, 5-6.11.2000, Boston, pp. 134-140.

[10] Matijević, D.V., Popović V.M.: Overview of modern contributions in vehicle noise and vibration refinement with special emphasis on diagnostics,

FME Transactions, Vol. 45, No. 3, pp. 448 - 458, 2017.

[11] Joseph, V.K.A., Thampi, G.: Engine block vibrations – an indicator of knocking in the SI engine, FME Transactions, Vol. 51, No. 3, pp. 395 - 403, 2023.

[12] BINH Le Khac, TUMA J.: Diagnostic internal combustion engine based on crankshaft angular acceleration, 2017. http://dsp.vscht.cz/konference_matlab/MATLAB11/prispevky/020_binh.pdf

[13] Yang, J., Pu, L., Wang, Z., Zhou, Y., Yan, X.: Fault detection in a diesel engine by analysing the instantaneous angular speed, Mechanical Systems and Signal Processing, Vol.15, No. 3, pp. 549-564, 2001.

[14] Osburn, A.W., Kostek, T.M., Franchek, M.A.: Residual generation and statistical pattern recognition for engine misfire diagnostics, Mechanical Systems and Signal Processing, Vol. 20, No. 8, pp. 2232-2258, 2006.

[15] Jaw, L.C., Lee, Y.-J.: Engine diagnostics in the eyes of machine learning, in: Proceedings of the ASME Turbo Expo, 16-20.06.2014, Dusseldorf, paper 6.

[16] Tuan Hoang, A., Nižetić, S., Chyuan Ong, H., Tarelko, W., Viet Pham, V., Hieu Le, T., Quang Chau, M., Phuong Nguyen, X.: A review on application of artificial neural network (ANN) for performance and emission characteristics of diesel engine fueled with biodiesel-based fuels, Sustainable Energy Technologies and Assessments, Vol. 47, No. 101416, 2021.

[17] Chen, J., Randall, R.: A vibration signal based simulation model for the misfire of Internal Combustion engines, in: *Proceedings of the 8th International Conference on Condition Monitoring and Machinery Failure Prevention Technologies*, 20–22.06.2011, Cardiff, pp. 659-671.

[18] Moskwa, J.J., Wang, W., Bucheger, D.J.: A new methodology for use in engine diagnostics and control, utilizing "synthetic" engine variables: Theoretical and experimental results, Journal of Dynamic Systems, Measurement and Control, Transactions of the ASME, Vol. 123, No. 3, pp. 528-534, 2001.

[19] Chang, J., Kim, M., Min, K.: Detection of misfire and knock in spark ignition engines by wavelet transform of engine block vibration signals, Measurement Science and Technology, Vol. 13, No. 7, pp. 1108-1114, 2002.

[20] Wu, J.-D., Chen, J.-C.: Continuous wavelet trans–form technique for fault signal diagnosis of internal combustion engines, NDT and E International, Vol. 39, No. 4, pp. 304-311, 2006.

[21] Sampath, S. et al.: Engine-fault diagnostics: An optimisation proce–dure, Applied Energy, Vol. 73, No. 1, pp. 47-70, 2002.

[22] Chen, J., Bond Randall, R.: Improved automated diagnosis of misfire in internal combustion engines based on simulation models, Mechanical Systems

and Signal Processing, Vol. 64-65, No. 3867, pp. 58-83, 2015.

[23] Gritsenko, A., Shepelev, V., Zadorozhnaya, E., Shubenkova, K.: Test diagnostics of engine systems in passenger cars, FME Transactions, Vol. 48, No.1, pp. 46-52, 2020.

[24] Gritsenko, A.V., Shepelev, V.D., Makarova, I.V.: Diagnostics of the fuel supply system of auto ICEs by the test method, Journal of King Saud University - Engineering Sciences, 2021 (in press).

[25] Filipi, Zoran S., Assanis, Dennis N.: Non-linear, transient, single-cylinder diesel engine simulation for predictions of instantaneous engine speed and torque, in: *Proceedings of the 1997 Spring Technical Conference of the ASME Internal Combustion Engine Division*, 27-30.04.1997, Fort Collins, pp. 61-70.

[26] Tinaut, F.V., Melgar, A., Laget, H., Domínguez, J.L.: Misfire and compression fault detection through the energy model, Mechanical Systems and Signal Processing, Vol. 21, No. 3, pp. 1521-1535, 2007.

[27] Dereszewski, M., Sikora, G.: Diagnostics of the internal combustion engines operation by measurement of crankshaft instantaneous angular speed, Journal of Konbin, Vol. 49, No. 4, pp. 281-295, 2020.

[28] Kazienko, D., Chybowski, L.: Instantaneous rotational speed algorithm for locating malfunctions in marine diesel engines, Energies, Vol. 16, No.3, Iss. 1396, 2020.

[29] USB Autoscope IV, automotive diagnostic oscilloscope and engine analyzer. http://autoscope.eu/home.

[30] Gritsenko, A., Shepelev, V., Lukomsky, K., Grakov, F., Kostyuchenkov, N., Kostyuchenkova, O.: Control of the exhaust gas tract resistance of modern engines by the rundown time during testing, Tribology in Industry, Vol. 42, No. 4, pp. 627-640, 2020.

NOMENCLATURE

α [-]	characterizes the change in the time components of acceleration
B [-]	characterizes the change in the time components of rundown
CPG	cylinder-piston group
DBD-4	gasoline engine reloader
d [mm]	diameter of the outlet pipe
$dt/d\omega$ [rad/s^2]	instantaneous acceleration value of the ICE crankshaft
ε_a [rad/s^2]	acceleration value during acceleration
ε_r [rad/s^2]	deceleration value during rundown
ICE	internal combustion engine
J [N·m^2]	moment of inertia reduced to the axis of the ICE crankshaft
K_{tc} [-]	coefficient
M_i [N·m]	indicated moment
M_t [N·m]	frictional moment
M_ε [N·m]	moment connected with an increase in

n [rpm]	crankshaft speed
N [rev]	total number of revolutions
t [s]	acceleration time
t_a [s]	point of free acceleration
t_r [s]	point of free rundown
ZMZ-4062	engine
Δt [s]	the difference in the rundown time between two adjacent dependencies increment or the degree of reduction of the ICE crankshaft speed (provided that
$\Delta\omega$ [rpm]	the same values of the greatest speeds are being considered during acceleration and rundown)
$\Delta\mu f$ [%]	injector capacity

the kinetic energy when the fuel supply increases

РАЗВОЈ МЕТОДЕ ЗА ДИЈАГНОСТИКОВАЊЕ МОТОРА СА УНУТРАШЊИМ САГОРЕВАЊЕМ НА ОСНОВУ КАРАКТЕРИСТИКА УБРЗАЊА И РАДА

А. Грисенко, В. Шепелев, А. Бурзев, Б.К. Калијев

У раду се предлаже примену прецизне и јефтине дијагностичке методе мотора са унутрашњим саго– ревањем (ИЦЕ) засноване на карактеристикама убрзања и рада. Развили смо штанд за тестирање мотора заснован на и одабраним дијагностичким алатима за снимање параметара убрзања: утова– ривач бензинског мотора ДБД-4 и УСБ Аутосцопе 4. Утврдили смо да брзина протока ињектора значајно утиче на време убрзања, док хабање цилиндра-клипна група (ЦПГ) значајно утиче на време убрзања ИЦЕ радилице. Када је хабање ЦПГ било 28%, време убрзања се повећало на 15 с, а када је хабање било 5% – на 3 с. Време заустављања значајно зависи од излазног отпора и повећава се са повећањем степена хабања ЦПГ-а. Примена развијене методе смањила је потрошњу горива тест мотора за 21%.